NANO LETTERS

pubs.acs.org/NanoLett

On-Chip Interferometric Detection of Nanomechanical Motion

Quirin P. Unterreithmeier, Thomas Faust, Stephan Manus, and Jörg P. Kotthaus*

Fakultät für Physik and Center for NanoScience (CeNS), Ludwig-Maximilians-Universität, Geschwister-Scholl-Platz 1, München 80539, Germany

ABSTRACT An integrable on-chip displacement transduction of nanomechenical motion is developed that senses the modulation of the optical near-field of an illuminated vibrating string with a nearby Schottky photodiode. This scheme poses no restrictions on resonator material and avoids additional damping. The achieved sensitivity of 1 pm/Hz$^{1/2}$ enables the detection of Brownian motion of our mechanical resonators at room temperature. Implementing a feedback scheme of the detected signal into the electrical actuation, we demonstrate self-oscillation.

KEYWORDS Nanomechanics, photodetection, motion detection, near-field interferometry, self-oscillation

The study of nanoelectromechanical systems (NEMS) is a rapidly evolving field of science, with implications ranging from fundamental science[1−5] to applications such as ultrasensitive systems detecting, e.g., mass,[6] temperature,[7] charge[8] or nuclear spins,[9] and signal generation[10] or processing.[11] Displacement detection schemes for such systems may be divided into two classes. One being optical interference techniques[1,3,12−14] which have the advantage of being material independent, yet usually require external components. The other utilizing on-chip components that transduce mechanical motion into modulated electrical signals,[2,15−20] with the inherent benefit of being integrable. The drawback of these techniques is their restriction to either low temperatures[2,15] and/or specific materials.[16−20] Here, we present a detection scheme that combines the local generation of the measurement signal and material independence. Our scheme is derived from the interferometric setup; there the mechanical resonator (and its surroundings) is illuminated and the reflected[21] or diffracted[22] beam is recollected. Mechanical displacement is converted into a modulation of the measured light intensity. Complementary to these schemes, we directly study the intensity modulation in the near-field of the resonator with a local photodiode, thereby creating an on-chip signal.

Figure 1a shows our setup: we study the displacement of a doubly clamped silicon nitride resonator of dimensions 35 μm × 100 nm × 200 nm (length, height, width, respectively). The utilized wafer consists of a typical sandwich structure: the substrate is n-doped (≈10 Ωcm) silicon that is partly oxidized, forming a 400 nm thick sacrificial layer. The device layer on top is composed of prestressed silicon nitride, leading to high mechanical quality factors[23] of, in this case, 10^5. The fabrication implements standard e-beam lithographic methods and subsequent reactive ion- and wet-etches to release the resonator. The wet-etch partly removes the silicon oxide with a remaining thickness of about 50 nm.

We electrically actuate our resonator via a pair of suitably biased electrodes processed on the postreleased structure nearby the resonator leading to an attractive dielectric force.[12,24] The high mechanical quality factor facilitates considerable displacements at low driving powers. A second pair of electrodes is processed with a small area in direct contact to the silicon substrate. This is accomplished by locally removing the SiO_2 employing another e-beam and wet etch step, leaving clearly visible depressions in the SiO_2,

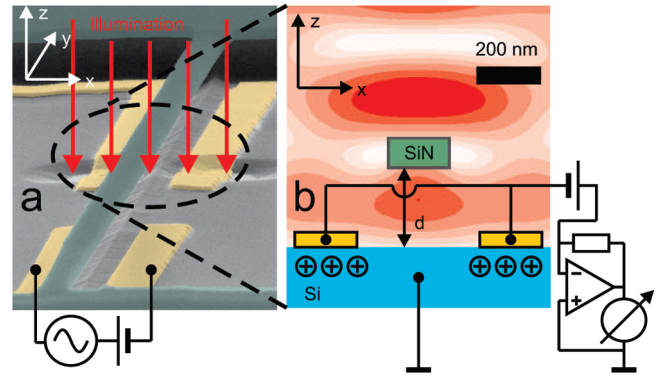

FIGURE 1. Setup and detection principle: (a) SEM picture (false color) of the sample; highlighted in green is the silicon nitride device layer forming the mechanical resonator and its supports. Two pairs of electrodes are marked in yellow; one pair serves as dielectric actuator, being suitably biased by dc and rf voltages. Small parts of the second electrode pairs are in direct contact with the silicon substrate, thereby forming a Schottky contact, as seen in the encircled area and in (b). Schematic cross section of the detection configuration; illumination (and suitably chosen bias) gives rise to a photocurrent that is detected using a current−voltage converter placed close to the sample. Interference and scattering lead to a nonuniform distribution of the resulting optical intensity in the near-field of the resonator; this intensity distribution is modulated by the displacement of the mechanical resonator, resulting in an rf part of the photocurrent.

* To whom correspondence should be addressed, kotthaus@lmu.de.
Received for review: 10/23/2009
Published on Web: 02/05/2010

DOI: 10.1021/nl903556s | *Nano Lett.* **2010,** *10,* 887–890

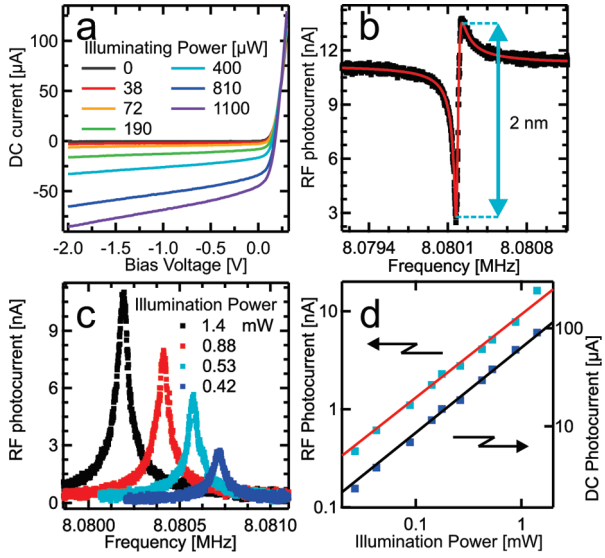

FIGURE 2. dc and rf photocurrent (diode laser illumination): (a) dc current traces vs applied voltage are displayed for different illumination powers, clearly exhibiting diode-like behavior. (b) Subject to actuation of the mechanical resonator, the rf part of the photocurrent is shown (black points). The resulting resonance can be excellently fitted using a Lorentzian superimposed by frequency-independent cross talk (red line). (c) Four rf resonances with mathematically subtracted cross talk are displayed, measured with different illumination powers. The resonance frequency is shifted by optical gradient forces. (d) The on-resonance rf photocurrent amplitude (light blue dots) and the dc photocurrent (dark blue dots) are depicted for illumination powers ranging over 2 decades. Both measurements can be seen to be proportional to the illumination power and with respect to each other, highlighted by the respective fits (red and black line).

as seen in Figure 1a. See Supporting Information for more geometric details. The thus formed Schottky contact causes depletion of the underlying silicon substrate, as indicated in Figure 1b. Illumination of a Schottky contact leads to the generation of mobile charges thus giving rise to a photocurrent. The illumination (coming from the top) forms a standing wave pattern, as sketched in Figure 1b, with the resulting optical near-field depending on the position of the mechanical resonator. As a consequence, the photocurrent is modulated with resonator displacement yielding the resonant signal. We employ the light of either a diode laser (DL, 670 nm) or a superluminescent diode (SLED, its wavelength is centered around 750 nm), coming out of the cleaved end of a bare glass fiber positioned above the resonator.[14] All our measurements are carried out under vacuum $<10^{-4}$ mbar at room temperature.

We now investigate the effect of (different) illumination; in our experiments an illumination power of 1 mW corresponds to an on-chip intensity of 6.4 W/mm^2. Figure 2a shows the typical dc current−voltage characteristics of the Schottky diode: with no illumination present the current is largely suppressed in reverse bias, i.e., at negative gate voltage; illumination leads to an enhanced (photo)current. We now actuate our mechanical resonator while sweeping the actuation frequency. The resulting rf part of the measured photocurrent is shown in Figure 2b. The sharp resonance corresponds to the mechanically induced rf photocurrent and is superposed by a frequency-independent background (cross talk). The latter we attribute to capacitive coupling of our actuation signal modulating the depletion region of the Schottky diode. The measured signal can be excellently fitted using a superposition of a Lorentzian line shape centered around the mechanical resonance frequency $f_0 \approx 8$ MHz and a flat background. The indicated displacement amplitude (in nanometers) is obtained as explained below. Please note that all amplitudes in this work are given as half-peak-to-peak values.

Figure 2c shows several such traces for different illumination powers; we mathematically subtract the cross talk resulting in the familiar Lorentzian lineshapes. Two effects arising from different illumination powers are clearly visible. Both the signal strength and the mechanical resonance frequency vary with the intensity. While the former is expected, the latter can be explained as a result of the illumination leading to an optical intensity pattern. As in the case of optical tweezers, see, e.g., ref 25, the resonator is attracted toward the region of larger light intensity. The influence on the mechanical resonance frequency results from the fact that this force is not uniform and hence its gradient counteracts in our geometry the intrinsic mechanical spring constant. This optical effect is in complete analogy to its dc dielectric counterpart employed in our actuation scheme.[12] To exclude heating effects, a model calculation can be found in the Supporting Information.

In order to compare the dc and rf part of the photocurrent, the intensity of the illumination is varied over almost 2 orders of magnitude. The rf amplitude on resonance and the dc part of the photocurrent are logarithmically plotted in Figure 2d. Both results are fitted with a power law ax^b, where x designates the light intensity and a and b are fit parameters. The slope of the curves yields the exponent b. Here the fit gives $b = 0.84$ and 0.86 for the rf and dc part, respectively, showing that both follow the same law. The slight deviation from linear behavior is assumed to reflect the reduction of the depletion zone with higher light intensities. The measurements of Figure 2 were performed using the DL, as it is experimentally easier to attenuate its intensity. Employing the SLED leads to virtually the same results with an additional advantage over the DL apart from setup complexity: in contrast to the output of our SLED, the DL is not externally intensity stabilized. As intensity fluctuations translate into fluctuations of the mechanical frequency, using the DL gives rise to undesirable additional fluctuations of the resonant displacement signal.

The high sensitivity of the setup allows us to directly measure the Brownian motion of our resonators. In Figure 3a we show the spectrum of the photocurrent without any rf actuation (measured with a bandwidth of 50 Hz). The thermally induced mean square displacement is predicted by theory $\langle x^2 \rangle = k_B T/(m_{eff}(2\pi f_0)^2)$ ($k_B T$ and m_{eff} are thermal

DOI: 10.1021/nl903556s | Nano Lett. 2010, 10, 887–890

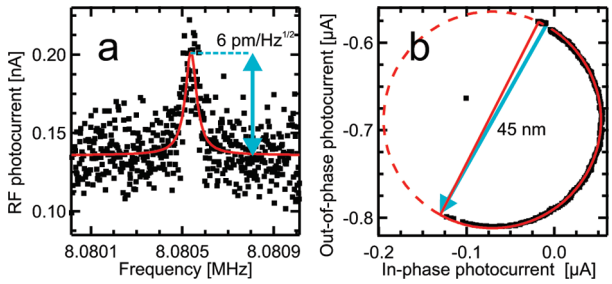

FIGURE 3. Sensitivity and linearity: (a) With no driving present, we measure (black dots) the rf photocurrent showing the Brownian motion of our mechanical resonator (measurement bandwidth, 50 Hz; DL illumination power, 0.8 mW; Schottky bias, 0 V). From theory (red line fit) we thereby obtain a factor to convert the measured signal into displacement. (b) Measurement (black dots) of a strongly actuated mechanical resonance, well within the nonlinear regime (SLED illumination power 1 mW and Schottky bias −2 V). The resulting rf photocurrent is plotted, divided into in- and out-of-phase components. As in the linear case, the measured points follow a circle, as shown by a fit (solid red line) and its continuation to a full circle (dashed red line). Thereby we can deduce that our detection scheme transduces displacements linearly up to amplitudes of 45 nm.

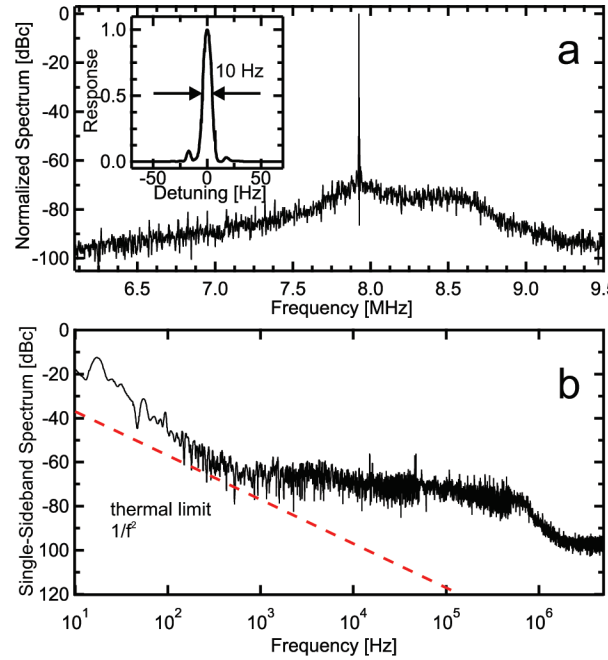

FIGURE 4. Suitably feeding back the displacement signal into the actuating electrodes, we obtain spontaneous oscillation of the resonator (SLED illumination power 1 mW, −2 V Schottky bias). (a) Measured power spectrum of the oscillator. The inset shows a zoom into the sharp resonance linearly plotted vs frequency. We attribute the shoulder visible in the spectrum to our not perfectly suppressed cross talk. (b) The single-sideband phase noise is shown (black line) in comparison to the theoretically predicted minimum (dashed line). For a discussion of the excess noise please see the main text.

energy and effective mass of the oscillatory mode, respectively); its frequency spectrum is fitted to the experimental data and enables us to convert the measured photocurrent into mechanical displacement[26] (also utilized in Figure 2b). Measuring with a 1 Hz bandwidth reduces the whole spectrum uniformly by a factor of $50^{1/2}$, then the maximum would correspond to an amplitude close to 1 pm/Hz$^{1/2}$, thus representing our estimate of sensitivity. As the noise floor is independent of applied bias across the Schottky diode and illumination power, we deduce that it is generated in the current−voltage converter.

Our measurement scheme avoids additional damping, i.e., preserves the unloaded quality factor. This is in contrast to "passive" schemes such as capacitive[20] or magnetomotive[4,5,10,11,16] detection. There the detection of Brownian motion at room temperature of a resonator with frequency $f_0 = 10$ MHz and an unloaded quality factor $Q = 1 \times 10^5$ degrades the quality factor by 10% when the signal power P exceeds $P = \Delta E f_0 = 0.1 k_B T/Q f_0 \approx 40$ zW (ΔE designates the energy loss per oscillation). The resulting signal corresponding to −164 dBm would be rather difficult to detect.

To check the linearity of the detection scheme, we measure the mechanical displacement subject to strong rf excitation. Figure 3b shows the in- and out-of-phase (quadrature) components of the rf photocurrent while sweeping the frequency. For a harmonic resonator this response is expected to move on a circle when sweeping over a resonance. Here, the measured response is statically shifted with respect to the origin because of the capacitive cross talk. Entering the nonlinear regime of this oscillator, this circular line is only followed in part until a sudden jump to lower amplitude values occurs.[27] However, the circular line is clearly followed (no distortion is seen), demonstrating the linearity of the detection scheme up to amplitudes of 45 nm.

Having characterized our detection scheme, we now demonstrate its applicability to implement a feedback-induced nanomechanical (self) oscillator,[10] here operating at room temperature. To obtain such self-oscillation, the detected displacement signal has to be suitably phase shifted, amplified, and fed back into the actuation. In order to suppress unwanted oscillations arising from the on-chip cross talk, a compensation line is introduced to minimize cross talk close to the mechanical resonance frequency. In addition, a bandpass filter is employed to eliminate off-resonant cross talk. Figure 4a shows the resulting power spectrum of the oscillator, biased only by a dc voltage. In the region around the resonance frequency, a prominent maximum dominates the nearly flat background signal. Its narrow line width of only about 10 Hz as visible in the inset is a characteristic of spontaneous feedback-stabilized oscillation. Compared to the case of the directly driven resonator, this represents a narrowing by a factor 8. In Figure 4b the power spectrum is plotted vs the frequency difference, often referred to as phase noise. On the basis of a simple model, see, e.g., ref 28, the theoretical minimum has been shown to have a slope of −20 dB per decade. In the range of approximately 10−500 Hz the observed slope appears to be steeper, possibly resulting from up-converted flicker noise.[10] We attribute the shoulder visible in the spectrum ranging approximately from 1 to 500 kHz to the not com-

DOI: 10.1021/nl903556s | *Nano Lett.* **2010,** *10,* 887–890

pletely suppressed cross talk, because its frequency range and shape (visible also in Figure 4a) match the frequency response of the employed bandpass filter intended to suppress the cross talk.

In conclusion, we established a new near-field detection scheme employing an on-chip Schottky photodiode and globally illuminated by light with low spatial coherence.[13] We are thereby able to reduce the external components necessary for the detection of the mechanical displacement of our nanoresonator to a mere illumination, making the scheme widely applicable. Superior to other utilized local detection schemes the near-field approach avoids appreciable loading the Q of the nanomechanical resonator. In addition, the detection scheme does not introduce any restrictions on resonator material such as conductivity.[4,5,10,11,16,20] We are able to measure the Brownian motion of our resonator at room temperature, achieving a sensitivity exceeding 1 pm/Hz$^{1/2}$. In addition, we demonstrate its versatility inducing self-oscillation providing a suitable feedback. It is noteworthy that this measurement scheme does not utilize down-conversion[19] or rf-reflection techniques,[29] both of which would make it less suitable as clock generator. Beyond the demonstrated performance, there is still plenty of room for improvements. The surrounding area of the mechanical resonator and the Schottky contact have not yet been optimized to yield a maximum photosignal with resonator displacement. Implementing a photonic cavitiy[3] or an optical near-field enhancement[25] seems straightforward. In addition, to realize an on-chip stand-alone clock, one would have to integrate the light source on-chip, a task that can be solved by either changing the substrate material or applying wafer bonding techniques.[30] One might even speculate that the signal generated in an optimized implementation of such a scheme would be strong enough to sustain self-oscillation without any additional amplification, thereby driven solely by the light source. Our detection scheme could also translate optically induced self-oscillation[31] into an on-chip electrical signal. Given recent demonstrations of operating nanomechanical resonators under ambient conditions,[32] the implementation of all these improvements could yield a completely integrable NEMS clock source. However, it remains to be shown whether the higher integrability and lower power consumption will outperform existing clock sources based on hybrid micromechanical systems.

Acknowledgment. Financial support by the Deutsche Forschungsgemeinschaft via project Ko 416/18 as well as the German Excellence Initiative via the Nanosystems Initiative Munich (NIM) and LMUexcellent is gratefully acknowledged.

Supporting Information Available. Additional information regarding device dimensions and heating of the beam. This material is available free of charge via the Internet at http://pubs.acs.org.

REFERENCES AND NOTES

(1) Anetsberger, G.; Arcizet, O.; Unterreithmeier, Q. P.; Riviere, R.; Schliesser, A.; Weig, E. M.; Kotthaus, J. P.; Kippenberg, T. J. *Nat. Phys.* **2009**, *5*, 909–914.
(2) LaHaye, M. D.; Buu, O.; Camarota, B.; Schwab, K. C. *Science* **2004**, *304*, 74–77.
(3) Eichenfield, M.; Camacho, R.; Chan, J.; Vahala, K. J.; Painter, O. *Nature* **2009**, *459*, 550–556.
(4) Kozinsky, I.; Postma, H. W. C.; Kogan, O.; Husain, A.; Roukes, M. L. *Phys. Rev. Lett.* **2007**, *99*, 207201.
(5) Aldridge, J. S.; Cleland, A. N. *Phys. Rev. Lett.* **2005**, *94*, 156403.
(6) Naik, A. K.; Hanay, M. S.; K, H. W.; Feng, X. L.; Roukes, M. L. *Nat. Nanotechnol.* **2009**, *4*, 445–450.
(7) Fon, W. C.; Schwab, K. C.; Worlock, J. M.; Roukes, M. L. *Nano Lett.* **2005**, *5*, 1968–1971.
(8) Cleland, A. N.; Roukes, M. L. *Nature* **1998**, *392*, 160.
(9) Mamin, H. J.; Poggio, M.; Degen, C. L.; Rugar, D. *Nat. Nanotechnol.* **2007**, *2*, 301–306.
(10) Feng, X. L.; White, C. J.; Hajimiri, A.; Roukes, M. L. *Nat. Nanotechnol.* **2008**, *3*, 342–346.
(11) Erbe, A.; Krommer, H.; Kraus, A.; Blick, R. H.; Corso, G.; Richter, K. *Appl. Phys. Lett.* **2000**, *77*, 3102–3104.
(12) Unterreithmeier, Q. P.; Weig, E. M.; Kotthaus, J. P. *Nature* **2009**, *458*, 1001–1004.
(13) Li, M.; Pernice, W. H. P.; Tang, H. X. *Nat. Nanotechnol.* **2009**, *4*, 377–382.
(14) Unterreithmeier, Q. P.; Manus, S.; Kotthaus, J. P. *Appl. Phys. Lett.* **2009**, *94*, 263104–3.
(15) Poggio, M.; Jura, M. P.; Degen, C. L.; Topinka, M. A.; Mamin, H. J.; Goldhaber-Gordon, D.; Rugar, D. *Nat. Phys.* **2008**, *4*, 635.
(16) Ekinci, K. L.; Yang, Y. T.; Huang, X. M. H.; Roukes, M. L. *Appl. Phys. Lett.* **2002**, *81*, 2253–2255.
(17) Bargatin, I.; Kozinsky, I.; Roukes, M. L. *Appl. Phys. Lett.* **2007**, *90*, No. 093116.
(18) Hüttel, A. K.; Steele, G. A.; Witkamp, B.; Poot, M.; Kouwenhoven, L. P.; van der Zant, H. S. J. *Nano Lett.* **2009**, *9*, 2547–2552.
(19) He, R.; Feng, X. L.; Roukes, M. L.; Yang, P. *Nano Lett.* **2008**, *8*, 1756–1761.
(20) Truitt, P. A.; Hertzberg, J. B.; Huang, C. C.; Ekinci, K. L.; Schwab, K. C. *Nano Lett.* **2007**, *7*, 120–126.
(21) Kouh, T.; Karabacak, D.; Kim, D. H.; Ekinci, K. L. *Appl. Phys. Lett.* **2005**, *86*, No. 013106.
(22) Thundat, T.; Finot, E.; Hu, Z.; Ritchie, R. H.; Wu, G.; Majumdar, A. *Appl. Phys. Lett.* **2000**, *77*, 4061–4063.
(23) Verbridge, S. S.; Parpia, J. M.; Reichenbach, R. B.; Bellan, L. M.; Craighead, H. G. *J. Appl. Phys.* **2006**, *99*, 124304.
(24) Schmid, S.; Wendlandt, M.; Junker, D.; Hierold, C. *Appl. Phys. Lett.* **2006**, *89*, 163506.
(25) Grigorenko, A. N.; Roberts, N. W.; Dickinson, M. R.; Zhang, Y. *Nat. Photonics* **2008**, *2*, 365–370.
(26) Gillespie, D. T. *Am. J. Phys.* **1996**, *64*, 225–240.
(27) Yurke, B.; Greywall, D. S.; Pargellis, A. N.; Busch, P. A. *Phys. Rev. A* **1995**, *51*, 4211–4229.
(28) Gonzales, G. *Foundations of Oscillator Circuit Design*; Artech House: Boston, MA, 2007.
(29) Regal, C. A.; Teufel, J. D.; Lehnert, K. W. *Nat. Phys.* **2008**, *4*, 555.
(30) Funato, M.; Fujita, S.; Fujita, S. *Appl. Phys. Lett.* **2000**, *77*, 3959–3961.
(31) Zalalutdinov, M.; Zehnder, A.; Olkhovets, A.; Turner, S.; Sekaric, L.; Ilic, B.; Czaplewski, D.; Parpia, J. M.; Craighead, H. G. *Appl. Phys. Lett.* **2001**, *79*, 695–697.
(32) Verbridge, S. S.; Bellan, L. M.; Parpia, J. M.; Craighead, H. G. *Nano Lett.* **2006**, *6*, 2109–2114.

DOI: 10.1021/nl903556s | *Nano Lett.* **2010,** *10,* 887–890